

Mechanism of quasi-phase-matching in a dual-gas multijet array

Xiaowei Wang,^{1,2} Michael Chini,¹ Qi Zhang,¹ Kun Zhao,¹ Yi Wu,¹ Dmitry A. Telnov,³ Shih-I Chu,⁴ and Zenghu Chang^{1,*}¹CREOL and Department of Physics, University of Central Florida, Orlando, Florida 32816, USA²Department of Physics, National University of Defense Technology, Changsha, Hunan 410073, China³Department of Physics, St. Petersburg State University, St. Petersburg 198504, Russia⁴Department of Chemistry, University of Kansas, Lawrence, Kansas 66045, USA

(Received 28 June 2012; published 31 August 2012)

Quasi-phase-matching in a dual gas (Ar-H₂) multijet array has recently been demonstrated to be a promising way to enhance the yield of high-order harmonics (HH). Here, we investigate the HH produced individually from these two gases under identical conditions. Our results indicate that the quasi-phase-matching results from the much lower recombination cross section of H₂ as compared to that of Ar in the energy range of interest, rather than from full ionization of H₂ by the driving laser as proposed previously.

DOI: [10.1103/PhysRevA.86.021802](https://doi.org/10.1103/PhysRevA.86.021802)

PACS number(s): 42.65.Ky, 31.15.E-, 33.15.Ry

Development of high-flux attosecond laser pulses for performing nonlinear optics and attosecond pump-attosecond probe experiments has attracted much interest in recent years [1–3]. In order to overcome the low conversion efficiency ($\sim 10^{-6}$) from the near-infrared (NIR) driving laser to the extreme ultraviolet (XUV) attosecond pulse, various techniques have been attempted, such as loose focusing [4], use of 400 nm driving lasers [3,5], and various quasi-phase-matching (QPM) techniques [6–8]. However, the highest achievable pulse energies to date have been on tens of microjoule level for attosecond pulse trains [4] and on the few-nanojoule level for isolated attosecond pulses [9].

One attractive candidate for QPM in a loose-focusing geometry is the use of an array of multiple high-order harmonics (HH) generation gas targets [8,10]. Recently, the generation of HH from multiple argon (Ar) gas jets separated by molecular hydrogen (H₂) “buffer” jets was shown to result in an enhancement of the HH yield by a factor of N^2 , where N is the number of Ar jets [10,11]. It was observed that by adjusting the backing pressure of the H₂ jets, quasi-phase-matching could be achieved. The authors argued that the H₂ is much more easily ionized by the driving laser due to its lower ionization potential compared to Ar, and that the H₂ was fully ionized by the leading edge of the driving laser pulse and did not generate HH in the most intense part of the laser pulse. Instead, the H₂ acted as a passive plasma medium, with the gas pressure chosen such that the XUV pulses produced from subsequent Ar jets add constructively. However, previous work on multiphoton and tunneling ionization of atoms and molecules reveals that H₂ is in fact more difficult to ionize than Ar [12,13], which invalidates the proposed mechanism [10,11]. Here, we investigate HH generated from H₂ and Ar gases individually. We find that under the same driving laser intensity and gas pressure, the HH yield of H₂ is approximately an order of magnitude less than that of Ar. We propose that the decreased yield of HH results from the low recombination cross section of H₂ as compared to Ar in the energy range of interest.

In the experiment, high-order harmonics were generated in a 1 mm long cell containing either Ar or H₂ gas. The driving laser pulse was 30 fs long with spectrum centered at 780 nm. The generated XUV beam was focused to a Ne gas target, and the photoelectron spectrum was measured by a magnetic bottle electron energy spectrometer (MBES) [14]. Due to the nearly constant photoionization cross section of Ne in the extreme ultraviolet and soft x-ray wavelength regions, the photoelectron spectrum serves as an energy-shifted replica of the HH spectrum. HH with photon energies between 20 eV and 75 eV were measured for different gas pressures and driving laser intensities.

We first investigated the HH yield from Ar and H₂ as a function of the target gas pressure, as shown in Fig. 1. The pressure inside the cell was the same for both Ar and H₂ under the same backing pressure, as verified by comparing the absorption of the generated HH in an identical cell with the known absorption cross sections of Ar and H₂ [15] and by gas flow simulations performed with FLUENT [16]. The laser intensity was $2.4(\pm 0.5) \times 10^{14}$ W/cm², as determined from the cutoff harmonic generated in Ne gas. Because the MBES has a detection limit ($\sim 10\,000$ electron counts/s), the pressure of the detection Ne gas jet was reduced for generation gas pressures above 20 torr, as indicated in the figure. Both Ar and H₂ exhibit a quadratic increase of the HH yield with increased gas pressure, which indicates that both Ar and H₂ are phase-matched as HH sources [17] when the pressure is less than 100 torr. The drop of the HH signal above 100 torr is likely due to the effects of the laser-produced plasma inside the generation target.

The results strongly indicate that the H₂ target is not fully ionized by the laser pulse at this intensity; otherwise the HH signal from H₂ would begin to decrease at much lower pressure than that from Ar. The similar roll-off pressure suggests that plasma density in the H₂ target is nearly the same as that in the Ar target. However, the QPM is still achievable due to the pressure dependence of the H₂ refractive index, which is different for the NIR driving laser and the HH. For partially ionized H₂, the refractive index can be estimated as [17]

$$n(\omega_q) \approx 1 + \frac{e^2 N}{2\epsilon_0 m_e} \left(\frac{1 - P}{\omega_r^2 - q^2 \omega_0^2} - \frac{P}{q^2 \omega_0^2} \right), \quad (1)$$

*zenghu.chang@ucf.edu

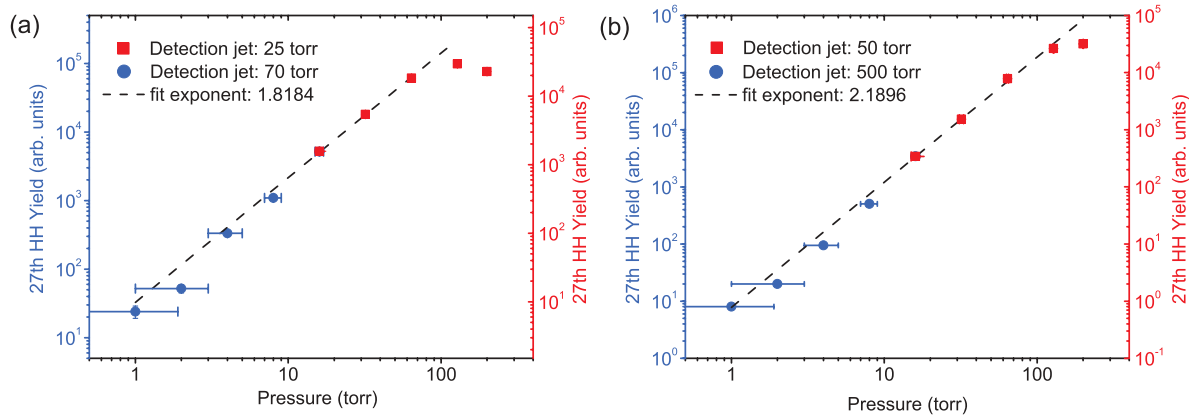


FIG. 1. (Color online) Dependence of the 27th HH on the generation gas pressure. (a) Ar and (b) H₂ can both be phase matched for pressure-length products up to approximately 100 torr × mm. The error is primarily due to determination of the pressure at low pressures.

where N is the H₂ molecular density which is related to the H₂ gas pressure, ω_0 is the frequency of the NIR driving laser, P is the ionization probability, and ω_r is the resonance frequency of the H₂ molecule. We can see that the refractive index for the NIR driving laser ($q = 1$) is a function of gas pressure and ionization probability, while for HH ($q \gg 1$), the refractive index $n(\omega_q) \approx 1$. The difference in the refractive index will lead to a phase difference between the NIR driving laser and HH after passing through the H₂ “buffer” jet. Furthermore, regardless of the ionization probability of H₂, the phase difference is always controllable by adjusting the gas pressure, and the QPM can be realized with a phase difference of $\pm\pi$.

We then compared the HH generated from Ar and H₂ under different driving laser intensities. The pressure in the generation gas cell was 5 torr for both Ar and H₂. The intensity within the focus was controlled using an iris, and was determined from the cutoff harmonic generated in Ne gas. Figure 2(a) shows the yield of the 19th harmonic (~ 30 eV) for different laser intensities from both experiment (symbols) and numerical modeling with the time-dependent density functional theory (TDDFT) (solid lines).

Traditionally many theoretical studies of multiphoton ionization (MPI) and HH generation (HHG) processes in molecules are based on various implementations of the strong-field approximation (SFA) and single-active-electron (SAE) model. However, while SFA-SAE-based models result in rather simple theoretical expressions, they fail to give quantitative agreement with more accurate theories. The discrepancy can be as large as several orders of magnitude. Besides other limitations, SFA-SAE-based theories usually deal only with the highest-occupied molecular orbital (HOMO) and neglect the multielectron dynamics of the target molecules. However, multielectron effects due to the electron exchange and correlation may be significant even when the inner electrons are strongly bound and are not excited by the driving laser field. Our theoretical method is based on the extension of TDDFT with proper long-range potentials (for a review, see [18]). The method takes into account the dynamic response of all the electron shells to the external fields and has been applied successfully to the nonperturbative study of MPI and HHG of atoms [19,20] and diatomic molecules [20,21] in intense laser fields. It is capable of reproducing the

Cooper minimum in the HH spectrum of Ar as well as the contributions of multiple orbitals to the HH generated from molecular gases. In the present TDDFT study, we make use of the LB94 exchange-correlation potential [22] which describes accurately the electronic structure of both Ar and H₂. Only hydrogen molecules with molecular axes aligned with the laser polarization were considered in the calculations.

In both the experiment and the simulation, the yield of the 19th HH is approximately an order of magnitude smaller for H₂ than for Ar, which is consistent with previous measurements [23]. The yield of the HH from Ar and H₂ are both observed to increase up to an intensity of $\sim 3 \times 10^{14}$ W/cm², where both gases have high ionization probability [13]. Above this intensity, ground-state depletion, plasma defocusing of the NIR laser in the generation target, and poor phase-matching

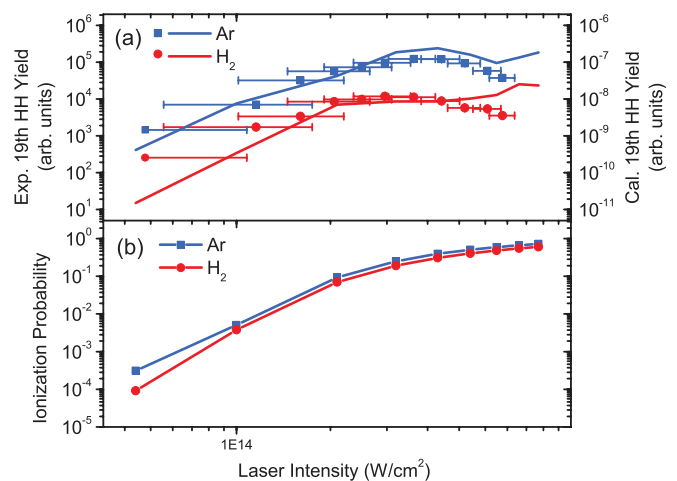


FIG. 2. (Color online) Scaling of HH with driving laser intensity. (a) Yields of 19th HH generated from Ar and H₂ increase with intensities up to $\sim 8 \times 10^{14}$ W/cm² (symbols, experimental results; solid lines, TDDFT calculation results). The error is primarily due to determination of the laser intensity from the cutoff harmonic generated from Ne gas. (b) Ionization probabilities of Ar and H₂ from TDDFT calculation. The ionization of H₂ is reduced compared to Ar up to intensities of $\sim (3-4) \times 10^{14}$ W/cm². The laser pulse assumed in the simulation was a cosine-squared pulse with a 30 fs FWHM duration centered at 780 nm.

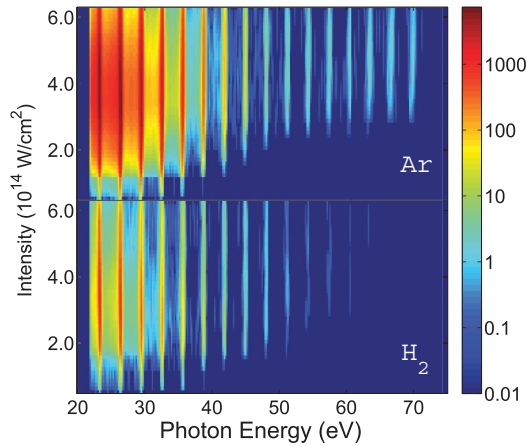


FIG. 3. (Color online) HH spectrum as a function of the laser intensity. Ar HH (upper) extends to the aluminum filter transmission edge. The HH signal from H₂ is lower than that from Ar in the entire spectrum and laser intensity range.

cause the HH yield to decrease. To verify this, the ionization probabilities for H₂ and Ar were also simulated in the TDDFT calculations, as shown in Fig. 2(b). For laser intensities above $\sim 3 \times 10^{14}$ W/cm², the ionization probabilities of both H₂ and Ar become close to unity. For lower intensities, the ionization probability of H₂ is always smaller than that of Ar in spite of its lower ionization potential, which is consistent with previous experiments [12,13]. Therefore, H₂ cannot be fully ionized at intensities for which HH generated from Ar is fully phase-matched in the multijet configuration.

In fact, the quasi-phase-matched buildup of HH observed by Willner [10] does not require that the H₂ target be fully ionized, but only that the H₂ gas does not efficiently generate or absorb the HH. In Fig. 2, we observed that the yield of the 19th harmonic generated in H₂ was approximately an order of magnitude smaller than that of Ar for all intensities. Figure 3 shows the HH spectrum measured as a function of the driving laser intensity. As the laser intensity increases, the cutoff energy of harmonics generated from Ar increases up to the limit of the aluminum filter transmission (~ 73 eV), which is well predicted by the semiclassical cutoff law for HHG [24]. At high intensities, HH signal from Ar could also be observed above the aluminum transmission edge by using a titanium filter. However, the yield of HH generated from H₂ gas was observed to be very low above ~ 60 eV, and no harmonics could be observed extending above the aluminum transmission edge. In the entirety of the measured photon energy and laser intensity range, the strength of HH generated from Ar is always much higher than that from H₂, which is required by dual-gas quasi-phase-matching.

The yield of HH is also closely related to the recombination cross section of the generation gas [25]. In Fig. 4, the measured HH spectra from Ar and H₂ with laser intensity of 4×10^{14} W/cm² are compared with their respective photoionization cross sections (PICS) [15], which are proportional to the recombination cross sections. We observe that the spectrum of the HH follows the PICS of the target atom. Small deviations of the HH spectra in Fig. 4(b) from the photoionization cross section shown in Fig. 4(a) are likely due to the nonuniform transmission of the aluminum filter and variations in the PICS of the

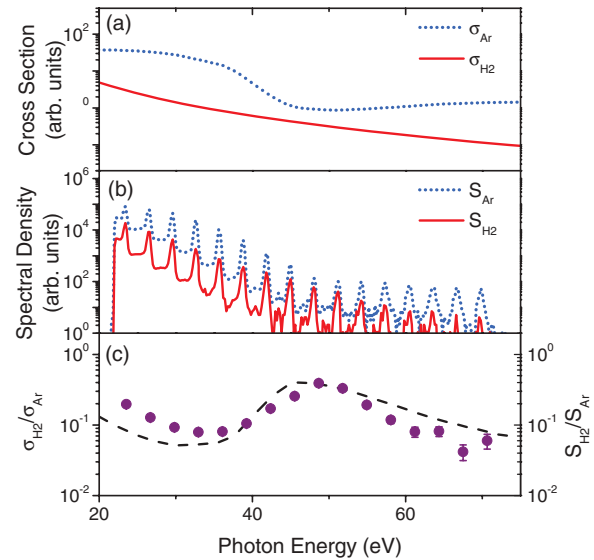


FIG. 4. (Color online) Cross-section dependence of HH yield. Comparison of (a) the photoionization cross sections with (b) the measured HH spectra. (c) Comparison of the cross-section ratio to the ratio of the spectrally resolved HH yields, eliminating the effects of the Al filter and detection gas. The error is primarily caused by the low signal levels of H₂ HH above 60 eV.

Ne detection gas. However, these effects are removed by taking the ratio of the harmonic spectra from the two gases, which is in good agreement with the PICS ratio shown in Fig. 4(c).

This dependence of the HH yield on the PICS explains two features observed in the HH spectrum generated in H₂. First, the reduced efficiency of H₂ HH (as well as the low absorption necessary for quasi-phase-matching) is largely due to the small recombination cross section. The PICS of H₂ is approximately an order of magnitude smaller than that of Ar in this energy range (except near the Cooper minimum at ~ 46 eV). Therefore, the HH yield of H₂ is negligible compared to that of Ar. Second, the lack of a HH signal from H₂ above ~ 70 eV is due to the reduced probability of recombination with such high photon energies. Whereas the PICS of Ar is nearly constant (or slightly increasing) above 50 eV, allowing observation of high-energy cutoff harmonics, the PICS of H₂ decreases by nearly an order of magnitude between 50 and 75 eV. Because of these features, QPM could be achieved in Ar using H₂ buffer gas, since the HH generated from H₂ is far too weak to destructively interfere significantly with that generated in Ar.

In conclusion, we find that under the same driving laser intensity and gas pressure, the yield of HH generated from H₂ gas is approximately an order of magnitude less than that from Ar. We propose that the relatively small recombination cross section of H₂ is responsible for the decreased yield of HH. Overall, H₂ exhibits low absorption of XUV light, low HH conversion efficiency, and tunable refractive index for the NIR driving laser, which allow it to be used as a passive medium for QPM of high-order harmonics generation. Although differing ionization rates may contribute to making this QPM scheme effective for certain gas pairings, such as He-H₂, it is not a general requirement. The proposed mechanism for QPM extends the usefulness of the dual-gas multijet array to gas

pairs other than Ar-H₂, for which the PICS of the buffer gas is low in the spectral range of interest.

This material is supported by the US Army Research Office and the National Science Foundation.

-
- [1] D. Charalambidis, P. Tzallas, E. P. Benis, E. Skantzakis, G. Maravelias, L. A. A. Nikolopoulos, A. Peralta Conde, and G. D. Tsakiris, *New J. Phys.* **10**, 025018 (2008).
- [2] E. J. Takahashi, P. Lan, O. D. Mucke, Y. Nabekawa, and K. Midorikawa, *Phys. Rev. Lett.* **104**, 233901 (2010).
- [3] S. D. Khan, Y. Cheng, M. Möller, K. Zhao, B. Zhao, M. Chini, G. G. Paulus, and Z. Chang, *Appl. Phys. Lett.* **99**, 161106 (2011).
- [4] Y. Nomura, R. Hörlein, P. Tzallas, B. Dromey, S. Rykovanov, Zs. Major, J. Osterhoff, S. Karsch, L. Veisz, M. Zepf, D. Charalambidis, F. Krausz, and G. D. Tsakiris, *Nat. Phys.* **5**, 124 (2009).
- [5] E. L. Falcão-Filho, C. Lai, K. Hong, V. M. Gkortsas, S. Huang, L. Chen, and F. X. Kärtner, *Appl. Phys. Lett.* **97**, 061107 (2010).
- [6] H. M. Milchberg, C. G. Durfee, and T. J. McIlrath, *Phys. Rev. Lett.* **75**, 2494 (1995).
- [7] X. Zhang, A. L. Lytle, T. Popmintchev, X. Zhou, H. C. Kapteyn, M. M. Murnane, and O. Cohen, *Nat. Phys.* **3**, 270 (2007).
- [8] J. Seres, V. S. Yakovlev, E. Seres, Ch. Strelis, P. Wobrauschek, Ch. Spielmann, and F. Krausz, *Nat. Phys.* **3**, 878 (2007).
- [9] F. Ferrari, F. Calegari, M. Lucchini, C. Vozzi, S. Stagira, G. Sansone, and M. Nisoli, *Nat. Photon.* **4**, 875 (2010).
- [10] A. Willner, F. Tavella, M. Yeung, T. Dzelzainis, C. Kamperidis, M. Bakarezos, D. Adams, M. Schulz, R. Riedel, M. C. Hoffmann, W. Hu, J. Rossbach, M. Drescher, N. A. Papadogiannis, M. Tatarakis, B. Dromey, and M. Zepf, *Phys. Rev. Lett.* **107**, 175002 (2011).
- [11] A. Willner, F. Tavella, M. Yeung, T. Dzelzainis, C. Kamperidis, M. Bakarezos, D. Adams, M. Schulz, R. Riedel, M. Schulz, M. C. Hoffmann, W. Hu, J. Rossbach, M. Drescher, V. S. Yakovlev, N. A. Papadogiannis, M. Tatarakis, B. Dromey, and M. Zepf, *New J. Phys.* **13**, 113001 (2011).
- [12] A. Talebpour, S. Larochelle, and S. L. Chin, *J. Phys. B* **31**, L49 (1998).
- [13] E. Wells, M. J. DeWitt, and R. R. Jones, *Phys. Rev. A.* **66**, 013409 (2002).
- [14] K. Zhao, Q. Zhang, M. Chini, and Z. Chang, *Multiphoton Processes and Attosecond Physics* (Springer-Verlag, Berlin, Germany, 2012).
- [15] http://henke.lbl.gov/optical_constants/.
- [16] ANSYS Fluent Flow Modeling Software, <http://www.fluent.com>.
- [17] Z. Chang, *Fundamentals of Attosecond Optics* (CRC, Boca Raton, FL, 2011).
- [18] Shih-I. Chu, *J. Chem. Phys.* **123**, 062207 (2005).
- [19] J. J. Carrera, Shih-I. Chu, and X. M. Tong, *Phys. Rev. A* **71**, 063813 (2005).
- [20] D. A. Telnov and Shih-I. Chu, *Phys. Rev. A* **80**, 043412 (2009).
- [21] J. Heslar, D. A. Telnov, and Shih-I. Chu, *Phys. Rev. A* **83**, 043414 (2011).
- [22] R. van Leeuwen and E. J. Baerends, *Phys. Rev. A* **49**, 2421 (1994).
- [23] C. Lynga, A. L'Huillier, and C. G. Wahlstrom, *J. Phys. B* **29**, 3293 (1996).
- [24] P. B. Corkum, *Phys. Rev. Lett.* **71**, 1994 (1993).
- [25] A. T. Le, R. D. Picca, P. D. Fainstein, D. A. Telnov, M. Lein, and C. D. Lin, *J. Phys. B* **41**, 081002 (2008).